Infrared Spectroelectrochemical Study of Dissociation and Oxidation of Methanol at Palladium Electrode in Alkaline Solution.

ARTICLE *in* LANGMUIR · JANUARY 2013

Impact Factor: 4.46 · DOI: 10.1021/la305141q · Source: PubMed

6 AUTHORS, INCLUDING:

Yao-Yue Yang
Southwest University for Nationalities
10 PUBLICATIONS **123** CITATIONS
SEE PROFILE

Zhi-You Zhou
Xiamen University
29 PUBLICATIONS **216** CITATIONS
SEE PROFILE

Wen-Bin Cai
Fudan University
111 PUBLICATIONS **2,113** CITATIONS
SEE PROFILE

Langmuir

Article

pubs.acs.org/Langmuir

Infrared Spectroelectrochemical Study of Dissociation and Oxidation of Methanol at a Palladium Electrode in Alkaline Solution

Yao-Yue Yang,[†] Jie Ren,[‡] Han-Xuan Zhang,[†] Zhi-You Zhou,*[,‡] Shi-Gang Sun,[‡] and Wen-Bin Cai*[,†]

[†]Shanghai Key Laboratory of Molecular Catalysis and Innovative Materials, Department of Chemistry, Fudan University, Shanghai 200433, China

[‡]State Key Laboratory of Physical Chemistry of Solid Surfaces, Department of Chemistry, College of Chemistry and Chemical Engineering, School of Energy Research, Xiamen University, Xiamen 361005, China

Supporting Information

ABSTRACT: The dissociative adsorption and electrooxidation of CH_3OH at a Pd electrode in alkaline solution are investigated by using in situ infrared spectroscopy with both internal and external reflection modes. The former (ATR-SEIRAS) has a higher sensitivity of detecting surface species, and the latter (IRAS) can easily detect dissolved species trapped in a thin-layer-structured electrolyte. Real-time ATR-SEIRAS measurement indicates that CH_3OH dissociates to CO_{ad} species at a Pd electrode accompanied by a "dip" at open circuit potential, whereas deuterium-replaced CH_3OH doesn't, suggesting that the breaking of the C−H bond is the rate-limiting step for the dissociative adsorption of CH_3OH. Potential-dependent ATR-SEIRAS and IRAS measurements indicate that CH_3OH is electrooxidized to formate and/or (bi)carbonate, the relative concentrations of which depend on the potential applied. Specifically, at potentials negative of ca. −0.15 V (vs Ag/AgCl), formate is the predominant product and (bi)carbonate (or CO_2 in the thin-layer structure of IRAS) is more favorable at potentials from −0.15 to 0.10 V. Further oxidation of the CO_{ad} intermediate species arising from CH_3OH dissociation is involved in forming (bi)carbonate at potentials above −0.15 V. Although the partial transformation from interfacial formate to (bi)carbonate may be justified, no bridge-bonded formate species can be detected over the potential range under investigation.

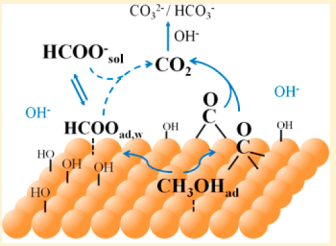

1. INTRODUCTION

The electrooxidation of small alcohol molecules at catalytic surfaces is an important fundamental topic owing to its relevance to the anode process of direct alcohol fuel cells (DAFCs) that currently use rare and expensive Pt-based catalysts in acidic media.[1,2] Nowadays, there is growing interest in developing alkaline polymer electrolyte fuel cells using less costly Pd-based catalysts, in consideration of their much higher electrocatalytic activity toward alcohol oxidation in basic media than in acidic media.[3−6] In this regard, the mechanistic study of alcohol dissociation and oxidation at a Pd electrode in alkaline media is of great importance for designing new, efficient, and economic catalysts for next-generation DAFCs.

CH_3OH is the simplest alcohol molecule and a widely used organic fuel for conventional DAFCs.[7−15] The self-dissociation and electrooxidation of CH_3OH at Pt electrodes in both acidic and alkaline solutions have been extensively studied by using various techniques, including but not limited to traditional electrochemical techniques, differential electrochemical mass spectrometry (DEMS),[1,15−18] and in situ Fourier transform infrared spectroscopy (FT-IR)[9,19−23] and so on. In contrast, the corresponding study of Pd electrodes in alkaline media has received far less attention. The first and only infrared spectroscopic study on this issue is reported by Nishimura et al.,[24] who barely detected a weak CO band by using electrochemically modulated infrared reflection spectroscopy and polarization modulated infrared reflection−adsorption spectroscopy. By using potential-modulated UV−vis reflectance spectroscopy, Caram et al.[25] assigned a reflectivity change to the presence of adsorbed CO at Pd in CH_3OH-containing alkaline solution. Recently, HPLC,[26] ionic chromatography (IC), and NMR measurements[27] have been extended to ex situ probe the above anodic oxidation, suggesting that formate and carbonate species could be the reaction products. Nevertheless, because of the very limited in situ vibrational spectral information obtained so far, the dissociative adsorption and electrooxidation of CH_3OH at a Pd electrode in alkaline solution is open to investigation.

Technically, electrochemical infrared spectroscopy mostly works in two reflection modes (i.e., external reflection with a thin-layer electrolyte structure (denoted as IRAS) and internal reflection with an open electrolyte structure (denoted as ATR-SEIRAS)). ATR-SEIRAS is more sensitive in detecting surface species than IRAS whereas IRAS is more sensitive in detecting solution species trapped in the thin layer.[28,29] Although surface enhancement was also detected in IRAS in some cases,[30,31] the restricted mass transport and the possible interference of solution signals on surface signals are often concerns when it is applied alone to characterize surface species during reaction processes. For example, IRAS is unable to give the ν(O−H) band clearly for surface free H_2O at a CO-predosed Pt

Received: December 28, 2012

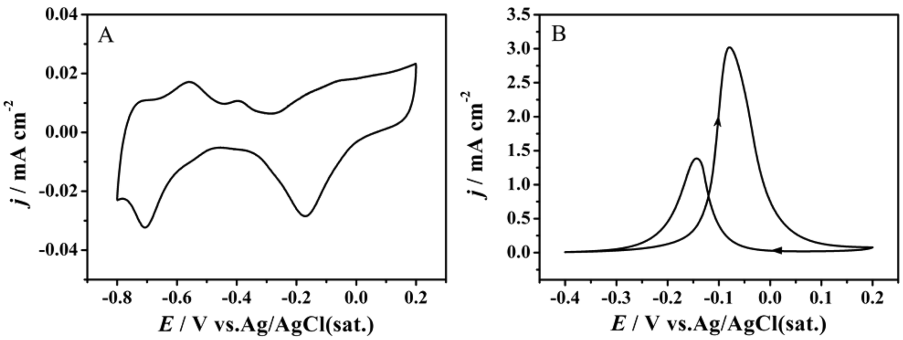

Figure 1. Cyclic voltammograms of the as-prepared Pd film electrode in deaerated 0.1 M NaOH solution (A) without and (B) with 0.5 M CH_3OH at a scan rate of 5 mV/s.

electrode.[32] However, despite the fact that ATR-SEIRAS has an advantage in detecting low-coverage or low-absorption surface species, the diffusion of low-concentration intermediates and products to the bulk solution during the reaction process mostly obscured them. Therefore, the combination of these two reflection modes is expected to provide richer in situ vibrational information about the electrocatalytic processes.

In the present work, ATR-SEIRAS and IRAS measurements are initially combined to investigate the self-dissociation and electrooxidation of CH_3OH at a Pd electrode in NaOH solution. The main purpose is to provide in situ spectral information about the intermediates and products existing at the Pd/electrolyte interface in order to get a better picture of the reaction pathways.

2. EXPERIMENTAL SECTION

2.1. ATR-SEIRAS. The Pd film working electrode was prepared according to the so-called "two-step wet process" developed in this group involving the initial chemical deposition of a ca. 60-nm-thick Au underfilm followed by the electrodeposition of a 30-nm-thick Pd overfilm.[33,34] Notably, to improve the adhesiveness between the Au underfilm and the Si reflecting surface in basic media, first a thinner Au film was dissolved in fresh aqua regia before the Si surface was reimmersed in the Au plating bath for a second deposition. The pinhole-free Pd overfilm was electrochemically cleaned by cycling the electrode potential between −0.8 and 0.2 V in 0.1 M NaOH versus Ag/AgCl(sat) until a reproducible cyclic voltammogram (CV) was obtained.

The Si prism with the working electrode was assembled into a spectroelectrochemical cell, and then it was fixed in a homemade optics system built in the chamber of a Varian FT3000 infrared spectrometer for electrochemical ATR-SEIRAS measurements at an angle of incidence of ca. 65°.[34] All ATR-SEIRAS spectra were shown in absorbance defined as $-\log(R/R_0)$, where R and R_0 represent the sample and reference spectra, respectively. Unless otherwise stated, the spectra taken in neat 0.1 M NaOH and CH_3OH-containing 0.1 M NaOH were used as the reference and sample spectra, respectively. Except for a special description, the acquisition time for each single-beam spectrum in each real-time successive measurement is 5 s (ca. 30 interferograms) at a spectral resolution of 8 cm^{-1}.

2.2. IRAS. A polycrystalline Pd disk (ø = 5 mm) embedded in a Teflon holder was used as the working electrode. Prior to measurements, the Pd electrode was polished successively with 1, 0.3, and 0.05 μm alumina powder and rinsed thoroughly with ultrapure water. Then, it was also electrochemically cleaned by potential cycling according to the aforementioned conditions.

In situ IRAS measurements were run on a Nicolet Nexus 870 spectrometer. The configuration of the thin-layer IR cell has been detailed previously.[35] In this configuration, unpolarized IR radiation was allowed to pass sequentially through a CaF_2 disc window (2 mm thickness) at an angle of incidence of about 55° and a thin-layer (ca. 10 μm) solution, and then it was reflected by the electrode surface, Thus, both dissolved species in the thin-layer solution and adsorbed species on the electrode surface can be detected. The resulting spectra were also reported in absorbance as mentioned above. To improve the signal-to-noise ratio (S/N) of the spectra, each spectrum was averaged over 1000 coadded interferograms at a spectral resolution of 8 cm^{-1}.

To reduce the impact of reactant consumption and product accumulation in the thin-layer solution, a single potential alternation FTIR (SPA-FTIR) method was employed.[36] According to this method, the thin-layer solution and electrode surface were renewed after the collection of one set of single-beam spectra at the reference potential (E_R) and sample potential (E_S) as the following clean procedures: first, the Pd electrode was lifted and the potential was held at 0.4 V for 5 s to oxidize any adsorbed species completely, and then the potential was stepped negatively to −0.75 V (E_R) to reduce the surface oxygen species but not oxidize the methanol; second, the Pd electrode was pushed against the CaF_2 IR window to form a new thin-layer solution, and the thickness of the thin-layer solution was controlled by the intensity of the reflected IR beam (deviation within 10%); and third, the single-beam spectra at the E_R and the next E_S were collected.

To reduce the effect of lowering the solution pH in the thin-layer solution by the release of protons during CH_3OH and surface oxidation processes, the concentration of CH_3OH was decreased from 0.5 M in ATR-SEIRAS to 0.1 M in the IRAS measurement.

2.3. IR Transmission Spectroscopy and Relative Concentrations of Products. A flow cell (Nicolet) was used for IR transmission spectra collection and consists of two CaF_2 disks spaced by a Teflon gasket of 6 μm thickness. For the purpose of semiquantitative analysis of the products in the thin layer at each potential, transmission spectra of a 0.1 M Na_2CO_3, 0.1 M $NaHCO_3$, and 0.1 M HCOONa solution and 0.034 M CO_2 (saturation solution) were collected, with the single-beam spectrum taken with pure water as the reference spectrum. A subtraction operation on in situ IRAS spectra with transmission spectra (that is, $C = A - kB$, where A is an in situ IRAS spectrum, B is a transmission spectrum, and k is a variable coefficient) was applied until the corresponding characteristic peaks (1390 cm^{-1} for CO_3^{2-}, 1360 cm^{-1} for HCO_3^-, 1580 and 1350 cm^{-1} for $HCOO^-$, and 2343 cm^{-1} for CO_2) disappeared in the in situ IRAS spectra. The obtained coefficient k could be used to calculate relative concentrations (C_r) of products according to $C_r = k \times 0.1$ M (but 0.034 M for CO_2), and the relative error is within 10% by this method. Here, the absolute concentration cannot be obtained because the optical paths are different for transmission and in situ IRAS measurements. More details about this semiquantitative analysis can be seen elsewhere.[35]

2.4. Other Conditions. A CHI 605B electrochemistry workstation was used for potential control and measurement of the current response. A Pt sheet and a Ag/AgCl with KCl saturated solution (denoted as Ag/AgCl(sat)) served as the counter and reference electrodes, respectively. The purity of D_2O, CD_3OD, or NaOD employed in isotope-labeled experiments is >99.99%. All other electrolytes were prepared with as-received GR-grade chemicals and

dx.doi.org/10.1021/la305141q | Langmuir XXXX, XXX, XXX−XXX

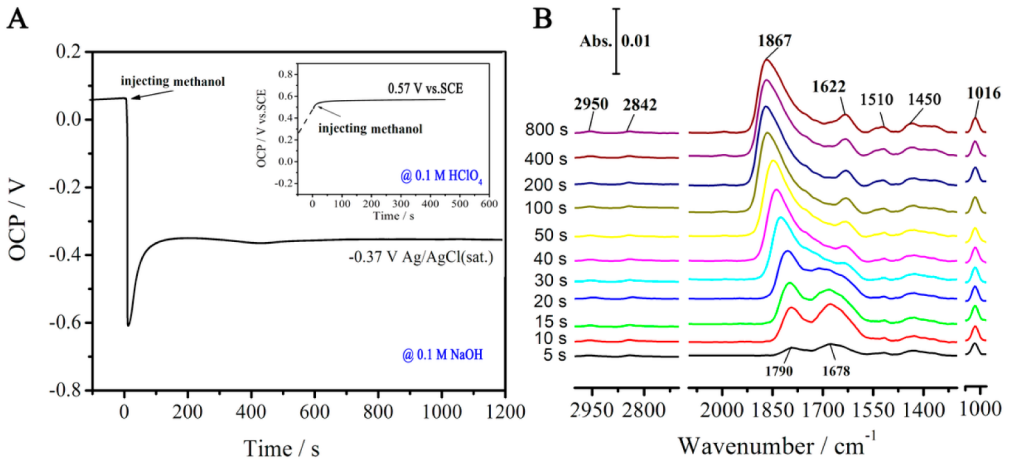

Figure 2. (A) Variation of OCP vs time caused by injecting CH_3OH into 0.1 M NaOH solution, where the inset displayed a similar measurment taken in 0.1 M $HClO_4$. (B) Real-time ATR-SEIRA spectra for a Pd film electrode in 0.1 M NaOH containing ca. 0.5 M CH_3OH, employing the single-beam spectrum taken in 0.1 M NaOH as the reference spectrum.

ultrapure Milli-Q water (≥18.2 MΩ·cm). They were deaerated thoroughly via bubbling high-purity Ar (99.999% purity). All measurements were carried out at room temperature.

3. RESULTS AND DISCUSSION

3.1. Cyclic Voltammetry. Figure 1A shows a cyclic voltammogram (CV) of the as-prepared Pd film electrode in a 0.1 M NaOH solution. On the basis of the previous investigations on single-crystalline and polycrystalline Pd electrodes in alkaline media,[37,38] a broad cathodic peak at around −0.1 V in the negative potential scan corresponds to the reduction of Pd (hydro)oxide formed during the preceding positive potential scan from −0.25 to 0.20 V, whereas the cathodic peak at −0.71 V can be attributed to the hydrogen absorption and adsorption. During the following positive scan, two broad anodic peaks are observed at −0.55 and −0.35 V, respectively. The former arises from the electrooxidation of absorbed and adsorbed hydrogen, and the latter contains contributions both from hydrogen desorption from the Pd surface and from oxygen-containing species adsorption at the Pd surface. As shown in Figure 1B, in the positive-going potential scan, the onset and peak oxidation potentials are located at ca. −0.35 and −0.06 V, respectively. The peak current density in the forward scan is almost twice that in the backward scan, although the peak potential in the former (−0.06 V) is slightly more positive than that in the latter (−0.14 V). This is due to a negligible contribution from the electrooxidation of CO_{ad} species in the negative scan with respect to that in the positive scan,[19] as suggested by our spectral results (vide infra). The oxidation current at the Pd electrode in Figure 1 is comparable to that at the Pt electrode in alkaline media.[39] Also notably, it is reported that the solution pH affects the electrocatalytic activity, the Pd electrode shows virtually negligible activity in acidic media (vide infra for more detailed discussion), and the best activity was reported in the solutions of pH 13 to 14.[38] In fact, Shen's group[40] proposed that a subtle balance of the alcohol and OH^- concentrations is required for high oxidation activity.

3.2. CH_3OH Self-Dissociation at the Pd Electrode. As can be seen from Figure 2A, after the addition of CH_3OH to 0.1 M NaOH the open circuit potential (OCP) of the Pd electrode experiences an initial decrease from 0.06 V down to −0.59 V at t = ca. 25 s and a subsequent slower rebound to ca. −0.38 V at ca. 175 s. The valley potential for the dip is already in the hydrogen adsorption potential region according to Figure 1A, suggesting that the formation of CO_{ad} species and Pd−H_{ad} is a result of CH_3OH self-dissociation. In contrast, the OCP of the Pd electrode was not shifted negatively when CH_3OH was added to the 0.1 M $HClO_4$, in stark contrast to that in 0.1 M NaOH (Figure 2A). This indicates that CH_3OH hardly dissociates at the Pd electrode in acidic media, in line with the previous DFT computation study of ethanol at the Pd electrode.[41] Figure 2B illustrates the real-time ATR-SEIRA spectra after the introduction of 0.5 M CH_3OH into 0.1 M NaOH, where we can see vibrational features of interfacial (including adsorbed) CH_3OH, adsorbed H_2O, and CO, as assigned in Table 1. Notably, the bands ranging from ca. 1678 to 1860 cm^{-1} in Figure 2B can be attributed to the combination of multibonded CO (CO_M) and bridge-bonded CO (CO_B) species, in harmony with those observed in the process of slowly dosing CO at a Pd electrode in 0.1 M $HClO_4$[34] and 0.1 M NaOH (Figure S1 in Supporting Information), where the vibrational frequency for CO_{ad} can be down to 1654 cm^{-1} at a given potential of −0.65 V vs Ag/AgCl(sat) in 0.1 M NaOH. It is worthwhile to notice that the CO_{ad} vibrational frequency shift chiefly arises from two causes according to the surface chemistry theory,[42] namely, the d−π back-donation from metal to CO_{ad} and the dipole−dipole coupling among CO_{ad} species. Usually, the d−π back-donation effect may be negligible at a given potential. Thus, the dipole−dipole coupling effect may better account for the blue shift of the CO_{ad} stretching frequency with increased CO dosing. Bands at 1510 and 1450 cm^{-1} may be assigned to the C−H bending vibration of adsorbed CH_3OH and/or CH_3O,[43] and these two

Table 1. Band Assignments in Figure 2B[a]

frequency/cm^{-1}	assignment
2949, 2841	ν(C−H) of surface CH_3OH and/or CH_3O[43]
1678−1860	ν(C−O) of CO_{ad}[34]
1622	δ(H−O−H) of H_2O_{free}[34]
1510, 1450	δ(C−H) of surface CH_3OH and/or CH_3O[43]
1016	ν(C−OH) of surface CH_3OH and/or CH_3O[19,43]

[a] ν, stretching vibration; δ, bending vibration.

dx.doi.org/10.1021/la305141q | Langmuir XXXX, XXX, XXX−XXX

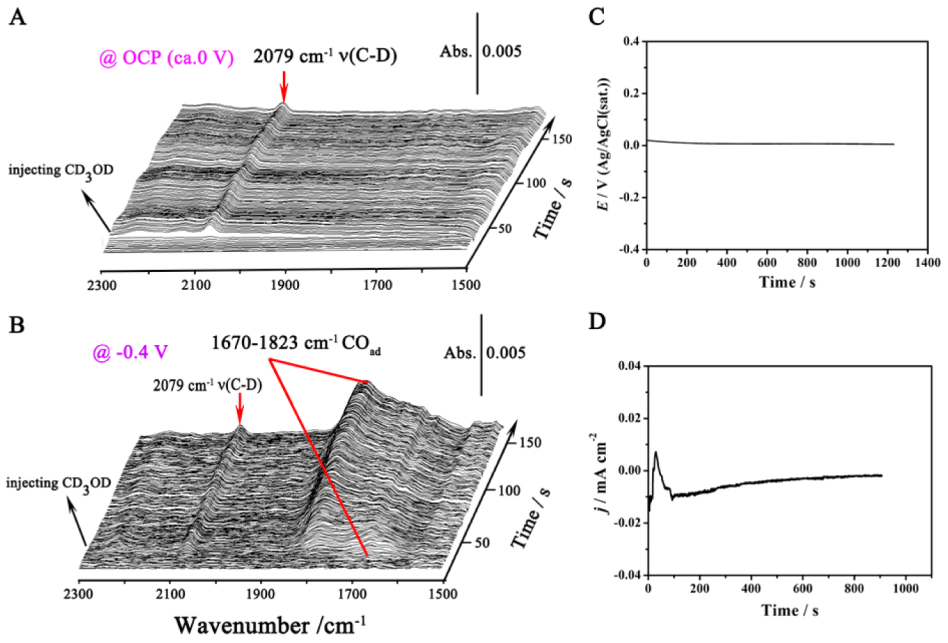

Figure 3. Real-time ATR-SEIRA spectra for a Pd film electrode with a 2 s^{-1} time resolution in 0.1 M NaOD D_2O solution containing ca. 0.5 M CD_3OD at (A) OCP and (B) −0.4 V. (C) Variation of OCP with time. (D) Current vs time response as the potential stepping from OCP to −0.4 V.

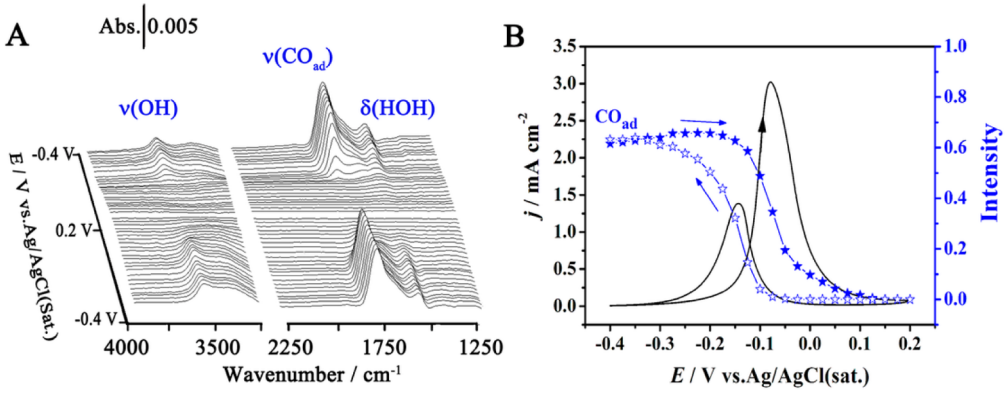

Figure 4. (A) Real-time ATR-SEIRA spectra measured on a Pd film electrode potential cycled between −0.4 and 0.2 V in 0.5 M CH_3OH + 0.1 M NaOH solution using the single-beam spectrum obtained at 0.2 V in the same solution as the reference spectrum. (B) Variations of CO_{ad} (solid blue ★, positive scan) (open blue ☆, negative scan) band intensity vs scan potential, together with the corresponding cyclic voltammogram (black solid line). The time resolution is 5 s, and all other conditions are the same as those in Figure 1B.

vibrational frequencies are somewhat higher than those for free CH_3OH.

With time spent, the CO band gains intensity with its frequency blue shifted to ca. 200 s, mirrored by the bounce in OCP to a rather stable value of ca. −0.37 V. It may be deduced that CH_3OH at a Pd surface in alkaline solution self-dissociates to form Pd−H and CO_{ad} species in a manner similar to the previously suggested stepwise dehydrogenation of CH_3OH at a Pt surface in acidic solution[7,44] and at Pd surface in UHV,[43,45,46] with relatively rapid dehydrogenation to form CH_3O_{ad} followed by relatively slow breaking of the C−H bond to form H_xCO_{ad} species and eventually rapid decomposition to CO_{ad} species.[45−47]

To confirm that the dehydrogenation step is also essential in the dissociation of CH_3OH to CO at the Pd electrode in alkaline media, an in situ ATR-SEIRAS measurement was carried out in D_2O solution containing 0.1 M NaOD and ca. 0.5 M CD_3OD. The reaction rate can be significantly modified if the isotope-substituted element participates in breaking or forming a chemical bond in the rate-limiting step. Hence, kinetic isotope effects (KIEs) have long been used to unravel mechanistic details in (electro)chemical reactions.[48−51] If the stepwise dehydrogenation is essential to the self-dissociation of CH_3OH to form CO_{ad}, then the deuteration should substantially slow down the process. Indeed, as can be seen from Figure 3C, after the addition of CD_3OD to 0.1 M NaOD in D_2O solution, a nearly unchanged OCP at around 0.02 V was observed, and no CO_{ad} feature band was detected between 1600 and 1900 cm^{-1} even after a rather long period of time, suggesting that virtually no Pd−D_{ad} is engendered at this OCP (and thus there is negligible breaking of the C−D bond) according to the cyclic voltammogram of the Pd film electrode in 0.1 M NaOD + D_2O solution (Figure S2). Only by lowering the potential to −0.4 V can we identify from Figure 3B the CO_{ad} formation (1670−1823 cm^{-1}) on a nominally reduced Pd surface in 0.1 M NaOD + D_2O. Because at an OCP of 0.02 V the Pd surface is partially covered with (hydro)oxide, only the more reactive C−H bond of CH_3O_{ad} can be broken, whereas

dx.doi.org/10.1021/la305141q | Langmuir XXXX, XXX, XXX−XXX

the less reactive C−D bond of CD_3O_{ad} may be broken only on a nominally reduced Pd surface. In other words, the KIEs further support the assumption that C−H bond breaking is the rate-limiting step for the dissociation of CH_3OH to form CO_{ad} at a Pd electrode in alkaline media.

3.3. CH_3OH Electrooxidation at a Pd Electrode. As mentioned above, the combination of ATR-SEIRAS and IRAS can provide richer molecular-level information of both adsorbed and dissolved species at the interface to assist in the mechanistic elucidation of CH_3OH electrooxidation at the Pd electrode in alkaline media.

To that end, an in situ ATR-SEIRAS measurement on the Pd electrode in 0.5 M CH_3OH-containing 0.1 M NaOH was conducted as the potential was scanned from −0.4 to 0.2 V and then back to −0.4 V. Figure 4 shows potential-dependent ATR-SEIRA spectra with reference to the single-beam spectrum acquired at 0.2 V. The bands due to surface CO_{ad} (1670−1860 cm^{-1}) and cohabitating H_2O_{free} (1620 cm^{-1} for δ(OH), 3604 cm^{-1} for ν(OH)) are clearly observed. As seen in Figure 4B, with the potential progressing positively, the CO_{ad} species starts to be electrooxidized at ca. −0.15 V and is then completely consumed at a potential above ca. 0.1 V, close to the anodic stripping of the adsorbed CO adlayer at the Pd electrode (Figure S3). The CO_{ad} species regenerates from CH_3OH adsorptive dissociation at ca. −0.05 V during the negative-going scan from the vertex potential of 0.2 V, accompanied by the reduction of the surface O-containing species (Figure 1A). The nominally reduced Pd surface favors the catalytic oxidation of CH_3OH at lower potentials as well as the accumulation of CO_{ad} species, which may explain the significant reduction of the oxidation current in the negative-going scan (cf. section 3.1). However, unlike the cases of CH_3OH at Pt[9,20] and HCOOH at Pd[34,52] in acid media, no ν_s(OCO) band for bridged-bonded formate was detected at ca. 1320−1230 cm^{-1} [19,19,34,52] and neither was the ν_{as}(OCO) band for adsorbed (bi)carbonate detected at 1400−1490 cm^{-1},[19,53−55] in spite of the significant SEIRA effect of the as-prepared Pd film (Figure S1). This indicates that the concentration of bridge-bonded formate or (bi)carbonate surface species, if any, is too low and beyond the limit of detection, probably because of the strong competitive adsorption of hydroxyl anions as suggested by Berna et al. on a Pd/Pt(111) electrode.[53] Nevertheless, bands characteristic of dissolved formate and (bi)carbonate were detected in the IRAS measurement of CH_3OH electrooxidation at the Pd electrode in NaOH solution via multistep acquisition as described in the Experimental Section. In Figure 5, the downward band at 1580 cm^{-1} from −0.35 V could be assigned to the ν_{as}(OCO) band of dissolved formate,[19,21] and the broad band located at 1300−1500 cm^{-1} from −0.35 V stems from the dissolved CO_3^{2-}/HCO_3^- and formate[19,21,53−55] in the thin-layer structure. As OH^- anions in the thin layer are partially neutralized by the protons released during the CH_3OH oxidation processes, ν_{as}(OCO) of dissolved CO_2 (downward, ca. 2343 cm^{-1}) can also be seen from −0.15 to 0.05 V. From the IRAS measurement, we may conclude that formate and (bi)carbonate (and/or CO_2 depending on the local pH) species are the main products of CH_3OH electrooxidation, in line with previous results based on HPLC,[26] IC, and NMR measurements.[27]

Although bridge-bonded formate was not detected over the whole potential range, the interfacial formate species on the solution side could serve as a reactive intermediate. Thermodynamically, $HCOO^-$ is readily oxidized to CO_3^{2-} at

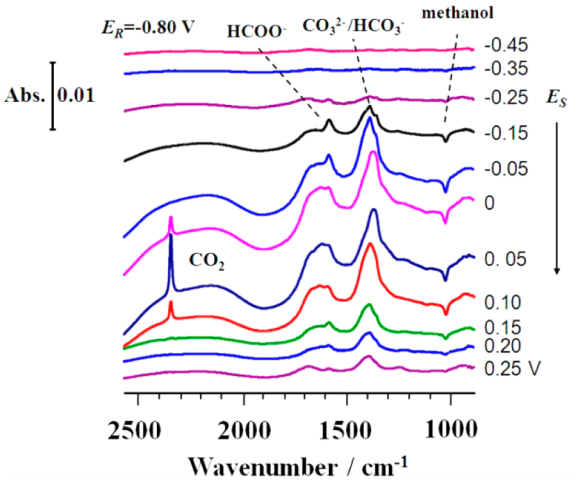

Figure 5. In situ IRAS spectra of CH_3OH electrooxidation at the Pd electrode at different potentials in 0.1 M NaOH + 0.1 M CH_3OH. E_S was varied from −0.45 to 0.25 V (vs Ag/AgCl(sat)), and E_R = −0.8 V (vs Ag/AgCl(sat)).

the Pd electrode in alkaline media over the applied potential range, in consideration of the following equations:[56−58]

$$HCOO^- + 3OH^- \rightarrow CO_3^{2-} + 2H_2O + 2e^-, \quad E^\Theta = -1.05\ \text{V(vs SHE)} \qquad (1)$$

Notably, ex situ analysis of the product components in the solution at different potentials by IC revealed that the concentration of the formate species decreases with the positive-going potential mirrored by an increase in the number of carbonate and bicarbonate species.[27] Our in situ IR spectral results may also suggest that the dual reaction pathways (i.e., CO_{ad} and interfacial formate serve as the two intermediates to form CO_2 and/or (bi)carbonates) may largely apply to the oxidation of CH_3OH at the Pd electrode in alkaline media, similar to the previously proposed reaction pathways for CH_3OH oxidation at the Pt electrode in both acidic and alkaline media.[9,19−21] Specifically, bridge-adsorbed formate species can be clearly identified at the Pt electrode in acidic solutions but not in alkaline solutions.[9,20]

In contrast, the Pd electrode shows virtually negligible activity in terms of methanol dissociation and oxidation in acidic media. First, the original OCP for the Pd electrode in 0.1 M $HClO_4$ was ca. 0.60 V (SCE) prior to a cathodic polarization at −0.2 V (SCE). Without potential control, the OCP gradually moved positively. The OCP of the Pd electrode was not shifted negatively when CH_3OH was added to 0.1 M $HClO_4$, in stark contrast to that in 0.1 M NaOH (Figure 2A). This indicates that CH_3OH hardly dissociates at the Pd electrode in acidic media, in line with the previous DFT computational study of ethanol at the Pd electrode.[41] Second, real-time electrochemical ATR-SEIRAS detected only a very low coverage of adsorbed CO species at lower potentials (1700−2000 cm^{-1}, Figure S5 in the Supporting Information) and interfacial carbonyl-containing species (such as formaldehyde with a weak, broad peak around 1700 cm^{-1}) at sufficiently high potentials as seen in Figure S4B in the Supporting Information, in association with insignificant CH_3OH electrooxidation at the Pd electrode in acidic media (Figure S4A in the Supporting Information). However, a comparable current for CH_3OH oxidation at the Pd electrode in basic media can be observed despite the fact that

dx.doi.org/10.1021/la305141q | Langmuir XXXX, XXX, XXX−XXX

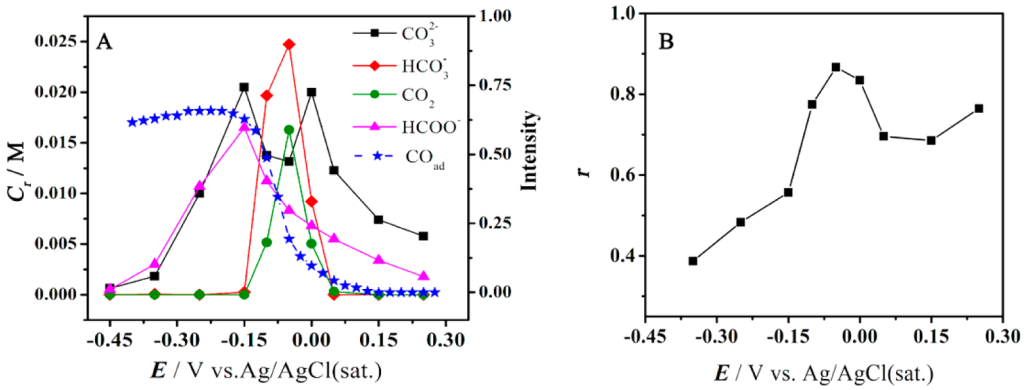

Figure 6. (A) Potential dependence of the relative concentration (C_r) of CO_3^{2-}, CO_2, $HCOO^-$, and HCO_3^- generated from CH_3OH oxidation at the Pd electrode and the CO_{ad} band intensity during the positive-going potential scan, adapted from Figure 4B. (B) Potential dependence of the selectivity (r) for complete CH_3OH oxidation to CO_2, HCO_3^-, and CO_3^{2-}.

the onset oxidation potential at the Pd electrode shifts positively by ca. 70 mV as compared to that at the Pt electrode.[39]

In the following text, we will further estimate the relative composition for each product in the electrolyte as a function of potential based on our IRAS measurement. The uplifting operation of the Pd electrode between two spectral collections during the multistep IRAS measurement was carried out to avoid the accumulation of reaction products formed at other potentials. The semiquantitative product analysis could be obtained by applying the subtraction of in situ IRAS spectra by the transmission spectra as mentioned in the Experimental Section.[35,55] As shown in Figure 6A, the relative concentration (C_r) of $HCOO^-$ increases sharply when the potential is greater than −0.35 V or the onset potential of CH_3OH electrooxidation at the Pd electrode (Figure 1B) attains a maximum at −0.15 V and then decreases. CO_3^{2-} is also detected between −0.35 and −0.15 V. Because detected CO_3^{2-} should not arise from the electrooxidation of CO_{ad} species at these lower potentials (Figures 4 and S3), we may deduce that a portion of as-produced formate species can be further oxidized to form carbonates between −0.35 and −0.15 V, which is in agreement with the hypothesis that formate may be a reactive or at least an important intermediate for the complete oxidation of CH_3OH.[9,21,52]

It should be pointed out that because of the thin-layer structure of the IRAS measurement the local pH tends to decrease because of the release of protons during the CH_3OH (and surface) oxidation processes with time at each potential as a result of the generation of CO_2. In fact, in addition to formate (the product of intermediate oxidation), the main products of complete oxidation including CO_2, CO_3^{2-}, and HCO_3^- are present in the thin layer, the relative amounts of which depend on the local pH and thus on the potential as well (Figure 5). Figure 6A also illustrates the potential-dependent C_r of CO_2, CO_3^{2-}, and HCO_3^-, and the selectivity for the complete oxidation of CH_3OH may be evaluated by introducing the parameter r that is defined as follows:

$$r = \frac{C_r(CO_3^{2-}) + C_r(HCO_3^-) + C_r(CO_2)}{C_r(CO_3^{2-}) + C_r(HCO_3^-) + C_r(CO_2) + C_r(HCOO^-)} \quad (2)$$

Figure 6B shows the relationship between r and the electrode potential. Formate is dominant at lower oxidation potentials (from −0.35 to −0.15 V), and CO_2 (including CO_3^{2-} and HCO_3^-) is the main product when the electrode potential is greater than −0.15 V. When E < −0.15 V, CO_{ad} species is not oxidized according to Figures 4 and 6, and only the formate species is produced (and some of this species is further oxidized), leading to a relatively low r value. When the potential is increased, the simultaneous electrooxidation of CO_{ad} and interfacial formate species contributes to the increase in the r value.

The electrooxidation of CH_3OH at the Pd electrode in an alkaline solution may be better illustrated in Scheme 1. CO_{ad} is generated by the stepwise dehydrogenation of surface CH_3OH and is electrooxidized to CO_2 at sufficiently high potentials. Meanwhile, the surface CH_3OH species is electrochemically oxidized to the intermediate product formate. Some of the interfacial formate species are further transformed to CO_2 or (bi)carbonate depending on the local pH, and the others diffuse into the bulk solution as a product of partial electrooxidation.

Scheme 1. Schematic Diagram for Surface CH_3OH Electrooxidation at the Pd Electrode in Alkaline Media[a]

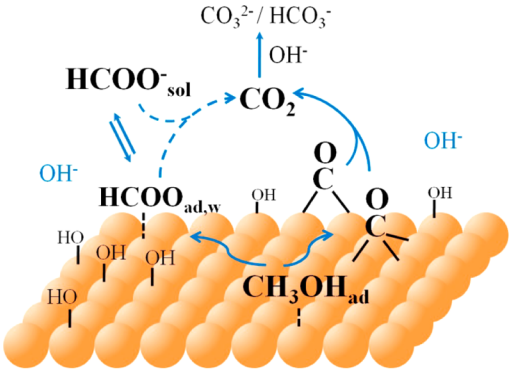

[a] $HCOO^-_{sol}$ and CH_3OH_{ad} represent dissolved formate and CH_3OH, respectively, and $HCOO_{ad,w}$ represents low-coverage, weakly adsorbed interfacial formates.

4. CONCLUSIONS

We have explored the dissociation and electrooxidation of CH_3OH at Pd electrodes in 0.1 M NaOH using electrochemical ATR-SEIRAS and IRAS methods. Spectral results without and with deuterium labeling have shown that CH_3OH can dissociate to form CO_{ad} at a Pd electrode at open circuit

dx.doi.org/10.1021/la305141q | Langmuir XXXX, XXX, XXX−XXX

potential as well as at potentials lower than ca. −0.10 V, involving the initial dissociation of the O−H bond followed by the stepwise cleavage of C−H bonds. On the basis of combined ATR-SEIRAS and IRAS measurements, a dual-pathway mechanism for complete CH_3OH oxidation to CO_2 (or (bi)carbonate) at the Pd electrode have been put forward, which involves CO_{ad} and interfacial formate as the intermediates. The formate is also the byproduct of incomplete CH_3OH oxidation. Moreover, the semiquantitative analyses of IRAS spectra have provided a potential-dependent (by)product distribution. The proposed reaction pathway at the Pd electrode is to some extent similar to that at the Pt electrode in alkaline media. Nevertheless, a higher potential is required to oxidize the two intermediates, and the conversion rate from formate to CO_2 (or (bi)carbonate) at the Pd electrode is less than that at the Pt electrode, leaving more formate in the solution as the byproduct in basic media. In acidic media, in contrast to an electrocatalytic oxidation of CH_3OH at a Pt electrode with surface-adsorbed formate being detected as the reactive intermediate, virtually no oxidation current or adsorbed formate can be observed at the Pd electrode. Pd exhibits the highest electrocatalytic activity toward methanol oxidation in basic media among the pure metals with the exception of much more expensive and much less abundant Pt, making it a promising potential anode catalyst in direct alkaline methanol fuel cells. Moreover, this work has demonstrated that the combination of ATR-SEIRAS and IRAS measurements is more reliable for elucidating the electrocatalytic reaction mechanism and thus may be regarded as a new development in electrochemical surface infrared spectroscopy.

■ ASSOCIATED CONTENT

Ⓢ Supporting Information

ATR-SEIRAS spectra showing the variation of CO adsorption sites at a Pd electrode with increased CO dosing. Cyclic voltammograms of a Pd film electrode in 0.1 M NaOD + D_2O solution and showing the anodic stripping of CO adsorbed at the Pd electrode in 0.1 M NaOH. Cyclic voltammograms and in situ ATR-SEIRA spectra at the Pd electrode in 0.1 M $HClO_4$ + 0.5 M CH_3OH. Comparison of IR spectra taken at Pd electrodes in 0.1 M NaOH + 0.5 M CH_3OH and 0.1 M $HClO_4$ + 0.5 M CH_3OH at 0.05 and 1.0 V (RHE). Transmission spectra of 0.1 M $NaCO_3$, 0.1 M $NaHCO_3$, and 0.1 M HCOONa solutions. This material is available free of charge via the Internet at http://pubs.acs.org.

■ AUTHOR INFORMATION

Corresponding Author

*E-mail: wbcai@fudan.edu.cn (C.W.B.); zhouzy@xmu.edu.cn (Z.Z.Y.).

Notes

The authors declare no competing financial interest.

■ ACKNOWLEDGMENTS

This work was supported by the NSFC (nos. 20833005, 21073045, and 21273046) and SMCST (nos. 11JC140200 and 08DZ2270500).

■ REFERENCES

(1) Lamy, C.; Belgsir, E. M.; Leger, J. M. Electrocatalytic oxidation of aliphatic alcohols: application to the direct alcohol fuel cell (DAFC). *J. Appl. Electrochem.* **2001**, *7*, 799.

(2) Vigier, F.; Rousseau, S.; Coutanceau, C.; Leger, J. M.; Lamy, C. Electrocatalysis for the direct alcohol fuel cell. *Top. Catal.* **2006**, *1*−*4*, 111.

(3) Antolini, E.; Gonzalez, E. R. Alkaline direct alcohol fuel cells. *J. Power Sources* **2010**, *11*, 3431.

(4) Bianchini, C.; Shen, P. K. Palladium-based electrocatalysts for alcohol oxidation in half cells and in direct alcohol fuel cells. *Chem. Rev.* **2009**, *9*, 4183.

(5) Antolini, E. Palladium in fuel cell catalysis. *Energy Environ. Sci.* **2009**, *9*, 915.

(6) Yin, Z.; Zhou, W.; Gao, Y. J.; Ma, D.; Kiely, C. J.; Bao, X. H. Supported Pd-Cu bimetallic nanoparticles that have high activity for the electrochemical oxidation of methanol. *Chem.—Eur. J.* **2012**, *16*, 4887.

(7) Iwasita, T. Electrocatalysis of methanol oxidation. *Electrochim. Acta* **2002**, *22*−*23*, 3663.

(8) Hamnett, A. Mechanism and electrocatalysis in the direct methanol fuel cell. *Catal. Today* **1997**, *4*, 445.

(9) Chen, Y. X.; Miki, A.; Ye, S.; Sakai, H.; Osawa, M. Formate, an active intermediate for direct oxidation of methanol on Pt electrode. *J. Am. Chem. Soc.* **2003**, *13*, 3680.

(10) Watanabe, M.; Motoo, S. Electrocatalysis by ad-atoms 2: enhancement of oxidation of methanol on platinum by ruthenium ad-atoms. *J. Electroanal. Chem.* **1975**, *3*, 267.

(11) Yajima, T.; Uchida, H.; Watanabe, M. In-situ ATR-FTIR spectroscopic study of electro-oxidation of methanol and adsorbed CO at Pt-Ru alloy. *J. Phys. Chem. B* **2004**, *8*, 2654.

(12) Gasteiger, H. A.; Markovic, N.; Ross, P. N.; Cairns, E. J. Temperature-dependent methanol electrooxidation on well-characterized Pt-Ru alloys. *J. Electrochem. Soc.* **1994**, *7*, 1795.

(13) Chrzanowski, W.; Wieckowski, A. Surface structure effects in platinum/ruthenium methanol oxidation electrocatalysis. *Langmuir* **1998**, *8*, 1967.

(14) Solla-Gullon, J.; Vidal-Iglesias, F. J.; Lopez-Cudero, A.; Garnier, E.; Feliu, J. M.; Aldaza, A. Shape-dependent electrocatalysis: methanol and formic acid electrooxidation on preferentially oriented Pt nanoparticles. *Phys. Chem. Chem. Phys.* **2008**, *25*, 3689.

(15) Housmans, T. H. M.; Wonders, A. H.; Koper, M. T. M. Structure sensitivity of methanol electrooxidation pathways on platinum: an on-line electrochemical mass spectrometry study. *J. Phys. Chem. B* **2006**, *20*, 10021.

(16) Cohen, J. L.; Volpe, D. J.; Abruna, H. D. Electrochemical determination of activation energies for methanol oxidation on polycrystalline platinum in acidic and alkaline electrolytes. *Phys. Chem. Chem. Phys.* **2007**, *1*, 49.

(17) Iwasita, T.; Vielstich, W. Online mass-spectroscopy of volatile products during methanol oxidation at platinum in acid-solutions. *J. Electroanal. Chem.* **1986**, *2*, 403.

(18) Wonders, A. H.; Housmans, T. H. M.; Rosca, V.; Koper, M. T. M. On-line mass spectrometry system for measurements at single-crystal electrodes in hanging meniscus configuration. *J. Appl. Electrochem.* **2006**, *11*, 1215.

(19) Zhou, Z. Y.; Tian, N.; Chen, Y. J.; Chen, S. P.; Sun, S. G. In situ rapid-scan time-resolved microscope FTIR spectroelectrochemistry: study of the dynamic processes of methanol oxidation on a nanostructured Pt electrode. *J. Electroanal. Chem.* **2004**, *1*, 111.

(20) Xue, X. K.; Wang, J. Y.; Li, Q. X.; Yan, Y. G.; Liu, J. H.; Cai, W. B. Practically modified attenuated total reflection surface-enhanced IR absorption spectroscopy for high-quality frequency-extended detection of surface species at electrodes. *Anal. Chem.* **2008**, *1*, 166.

(21) Christensen, P. A.; Linares-Moya, D. The role of adsorbed formate and oxygen in the oxidation of methanol at a polycrystalline Pt electrode in 0.1 M KOH: an in situ fourier transform infrared study. *J. Phys. Chem. C* **2010**, *2*, 1094.

(22) Spendelow, J. S.; Wieckowski, A. Electrocatalysis of oxygen reduction and small alcohol oxidation in alkaline media. *Phys. Chem. Chem. Phys.* **2007**, *21*, 2654.

(23) Lipkowski, J.; Ross, P. N. *Electrocatalysis*; Wiley-VCH: New York, 1998; p 1.

(24) Nishimura, K.; Kunimatsu, K.; Enyo, M. Electrocatalysis on Pd + Au alloy electrodes 3: IR spectroscopic studies on the surface species derived from CO and CH_3OH in NaOH solution. *J. Electroanal. Chem.* **1989**, *1*, 167.
(25) Caram, J. A.; Gutierrez, C. Cyclic voltammetric and potential-modulated reflectance study of the electroadsorption of CO, methanol and ethanol on a palladium electrode in acid and alkaline media. *J. Electroanal. Chem.* **1993**, *1−2*, 313.
(26) Santasalo-Aarnio, A.; Kwon, Y.; Ahlberg, E.; Kontturi, K.; Kallio, T.; Koper, M. T. M. Comparison of methanol, ethanol and iso-propanol oxidation on Pt and Pd electrodes in alkaline media studied by HPLC. *Electrochem. Commun.* **2011**, *5*, 466.
(27) Bambagioni, V.; Bianchini, C.; Marchionni, A.; Filippi, J.; Vizza, F.; Teddy, J.; Serp, P.; Zhiani, M. Pd and Pt-Ru anode electrocatalysts supported on multi-walled carbon nanotubes and their use in passive and active direct alcohol fuel cells with an anion-exchange membrane (alcohol = methanol, ethanol, glycerol). *J. Power Sources* **2009**, *2*, 241.
(28) Li, J. T.; Zhou, Z. Y.; Broadwell, I.; Sun, S. G. In-situ infrared spectroscopic studies of electrochemical energy conversion and storage. *Acc. Chem. Res.* **2012**, *4*, 485.
(29) Osawa, M. In *Handbook of Vibrational Spectroscopy*; Chalmers, J. M., Griffiths, P. R., Eds.; John Wiley & Sons: Chichester, U.K., 2002; Vol. *1*, p 785.
(30) Bjerke, A. E.; Griffiths, P. R.; Theiss, W. Surface-enhanced infrared absorption of CO on platinized platinum. *Anal. Chem.* **1999**, *10*, 1967.
(31) Lu, G. Q.; Sun, S. G.; Cai, L. R.; Chen, S. P.; Tian, Z. W.; Shiu, K. K. In situ FTIR spectroscopic studies of adsorption of CO, SCN^-, and poly(o-phenylenediamine) on electrodes of nanometer thin films of Pt, Pd, and Rh: abnormal infrared effects (AIREs). *Langmuir* **2000**, *2*, 778.
(32) Samjeske, G.; Komatsu, K.; Osawa, M. Dynamics of CO oxidation on a polycrystalline platinum electrode: a time-resolved infrared study. *J. Phys. Chem. C* **2009**, *23*, 10222.
(33) Yan, Y. G.; Li, Q. X.; Huo, S. J.; Ma, M.; Cai, W. B.; Osawa, M. Ubiquitous strategy for probing ATR surface-enhanced infrared absorption at platinum group metal-electrolyte interfaces. *J. Phys. Chem. B* **2005**, *16*, 7900.
(34) Wang, J. Y.; Zhang, H. X.; Jiang, K.; Cai, W. B. From HCOOH to CO at pd electrodes: a surface-enhanced infrared spectroscopy study. *J. Am. Chem. Soc.* **2011**, *38*, 14876.
(35) Zhou, Z. Y.; Chen, D. J.; Li, H.; Wang, Q.; Sun, S. G. Electrooxidation of dimethoxymethane on a platinum electrode in acidic solutions studied by in situ FTIR spectroscopy. *J. Phys. Chem. C* **2008**, *48*, 19012.
(36) Corrigan, D. S.; Leung, L. W. H.; Weaver, M. J. Single potential-alteration surface infrared-spectroscopy: examination of adsorbed species involved in irreversible electrode-reactions. *Anal. Chem.* **1987**, *18*, 2252.
(37) Hoshi, N.; Nakamura, M.; Maki, N.; Yamaguchi, S.; Kitajima, A. Structural effects on voltammograms of the low index planes of palladium and Pd(S)-[n(100) × (111)] surfaces in alkaline solution. *J. Electroanal. Chem.* **2008**, *1−2*, 134.
(38) Liang, Z. X.; Zhao, T. S.; Xu, J. B.; Zhu, L. D. Mechanism study of the ethanol oxidation reaction on palladium in alkaline media. *Electrochim. Acta* **2009**, *8*, 2203.
(39) Xu, C. W.; Cheng, L. Q.; Shen, P. K.; Liu, Y. L. Methanol and ethanol electrooxidation on Pt and Pd supported on carbon microspheres in alkaline media. *Electrochem. Commun.* **2007**, *5*, 997.
(40) Fang, X.; Wang, L. Q.; Shen, P. K.; Cui, G. F.; Bianchini, C. An in situ Fourier transform infrared spectroelectrochemical study on ethanol electrooxidation on Pd in alkaline solution. *J. Power Sources* **2010**, *5*, 1375.
(41) Cui, G. F.; Song, S. Q.; Shen, P. K.; Kowal, A.; Bianchini, C. First-principles considerations on catalytic activity of Pd toward ethanol oxidation. *J. Phys. Chem. C* **2009**, *35*, 15639.
(42) Rodriguez, J. A.; Goodman, D. W. The nature of the metal metal bond in bimetallic surfaces. *Science* **1992**, *5072*, 897.
(43) Collins, S. E.; Baltanas, M. A.; Bonivardi, A. L. Mechanism of the decomposition of adsorbed methanol over a Pd/α,β-Ga_2O_3 catalyst. *Appl. Catal., A* **2005**, *2*, 126.
(44) Bagotzky, V. S.; Vassiliev, Y. B.; Khazova, O. A. Generalized scheme of chemisorption, electrooxidation and electroreduction of simple organic-compounds on platinum group metals. *J. Electroanal. Chem.* **1977**, *2*, 229.
(45) Borasio, M.; de la Fuente, O. R.; Rupprechter, G.; Freund, H. J. In situ studies of methanol decomposition and oxidation on Pd(111) by PM-IRAS and XPS spectroscopy. *J. Phys. Chem. B* **2005**, *38*, 17791.
(46) Cabilla, G. C.; Bonivardi, A. L.; Baltanas, M. A. FTIR study of the adsorption of methanol on clean and Ca-promoted Pd/SiO_2 catalysts. *J. Catal.* **2001**, *2*, 213.
(47) Mellinger, Z. J.; Kelly, T. G.; Chen, J. G. Pd-modified tungsten carbide for methanol electro-oxidation: from surface science studies to electrochemical evaluation. *ACS Catal.* **2012**, *5*, 751.
(48) Wieckowski, A. Kinetic isotope effects between light and heavy-water in HCOOH and CH_3OH adsorption and oxidation on Pt mechanistic considerations. *J. Electroanal. Chem.* **1977**, *2*, 229.
(49) Chen, Y. X.; Heinen, M.; Jusys, Z.; Behm, R. J. Kinetic isotope effects in complex reaction networks: formic acid electro-oxidation. *ChemPhysChem* **2007**, *3*, 380.
(50) Holze, R.; Luczak, T.; Beltowskabrzezinska, M. The kinetic isotope effect in the oxidation of aliphatic-alcohols on a gold electrode. *Electrochim. Acta* **1994**, *4*, 485.
(51) Franaszczuk, K.; Herrero, E.; Zelenay, P.; Wieckowski, A.; Wang, J.; Masel, R. I. A comparison of electrochemical and gas-phase decomposition of methanol on platinum surfaces. *J. Phys. Chem.* **1992**, *21*, 8509.
(52) Miyake, H.; Okada, T.; Samjeske, G.; Osawa, M. Formic acid electrooxidation on Pd in acidic solutions studied by surface-enhanced infrared absorption spectroscopy. *Phys. Chem. Chem. Phys.* **2008**, *25*, 3662.
(53) Berna, A.; Rodes, A.; Feliu, J. M.; Illas, F.; Gil, A.; Clotet, A.; Ricart, J. M. Structural and spectroelectrochemical study of carbonate and bicarbonate adsorbed on Pt(111) and Pd/Pt(111) electrodes. *J. Phys. Chem. B* **2004**, *46*, 17928.
(54) Arihara, K.; Kitamura, F.; Ohsaka, T.; Tokuda, K. Characterization of the adsorption state of carbonate ions at the Au(111) electrode surface using in situ IRAS. *J. Electroanal. Chem.* **2001**, *1−2*, 128.
(55) Zhou, Z. Y.; Wang, Q. A.; Lin, J. L.; Tian, N.; Sun, S. G. In situ FTIR spectroscopic studies of electrooxidation of ethanol on Pd electrode in alkaline media. *Electrochim. Acta* **2010**, *27*, 7995.
(56) Nishimura, K.; Machida, K. I.; Enyo, M. Electrooxidation of formate and formaldehyde on electrodes of alloys between Pd and group-Ib metals in alkaline media 1: electrocatalytic properties of component metals. *J. Electroanal. Chem.* **1988**, *1*, 103.
(57) Takamura, T.; Mochimar., F. Adsorption and oxidation of formate on palladium in alkaline solution. *Electrochim. Acta* **1969**, *1*, 111.
(58) Bartrom, A. M.; Haan, J. L. The direct formate fuel cell with an alkaline anion exchange membrane. *J. Power Sources* **2012**, 68.

Supporting information

Infrared Spectroelectrochemical Study of Dissociation and Oxidation of Methanol at Palladium Electrode in Alkaline Solution

Yao-Yue Yang[†]; Jie Ren[‡]; Han-Xuan Zhang[†]; Zhi-You Zhou[‡]; Shi-Gang Sun[‡]; Wen-Bin Cai[†]**

†Shanghai Key Laboratory of Molecular Catalysis and Innovative Materials, Department of Chemistry, Fudan University, Shanghai 200433,China

‡State Key Laboratory of Physical Chemistry of Solid Surfaces, Department of Chemistry, College of Chemistry and Chemical Engineering, School of Energy Research, Xiamen University, Xiamen 361005,China

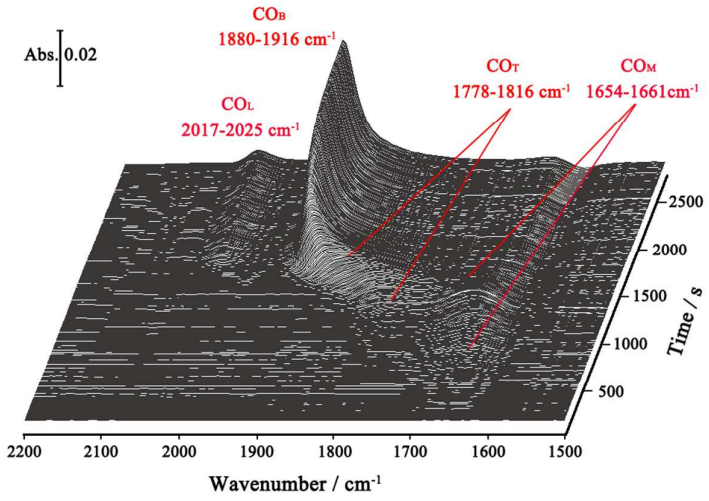

Figure S1. Time-evolved SEIRA spectra for a Pd electrode in 0.1 M NaOH solution recorded during controlled bubbling of diluted CO in Ar gas (CO: Ar = 1:5) at -0.65 V. The spectrum collected in neat 0.1 M NaOH solution was taken as the reference spectrum. Each spectrum was acquired for 5 s at a spectral resolution of 8 cm^{-1}.

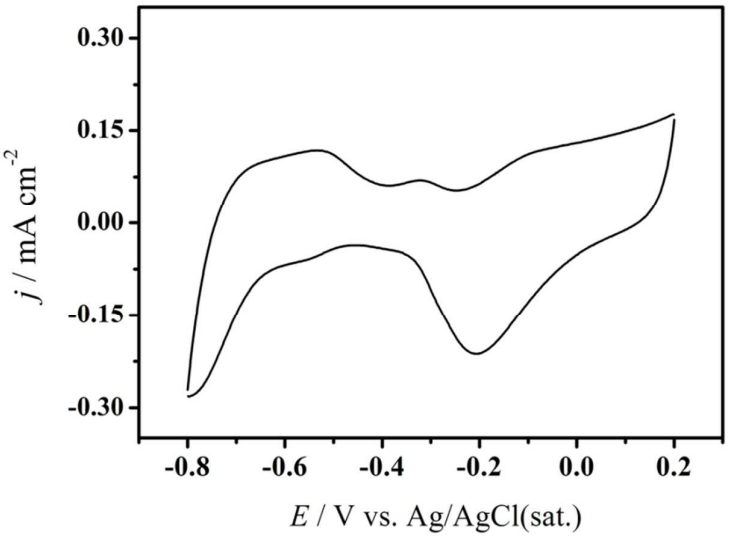

Figure S2. Cyclic voltammogram for a Pd film electrode in 0.1 M NaOD + D_2O solution at 50 mV/s.

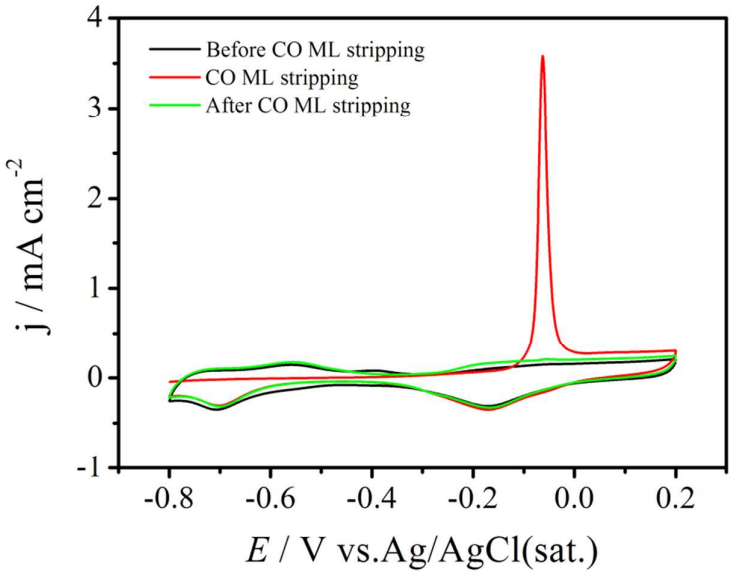

Figure S3. Cyclic voltammograms for anodic stripping of CO monolayer (CO ML) adsorbed at Pd film electrode in 0.1 M NaOH at 50 mV/s. CO was predosed at Pd electrode by bubbling CO into the electrolyte for 20 min followed by purging dissolved CO with a high purity Ar flow for 20 min at -0.6 V.

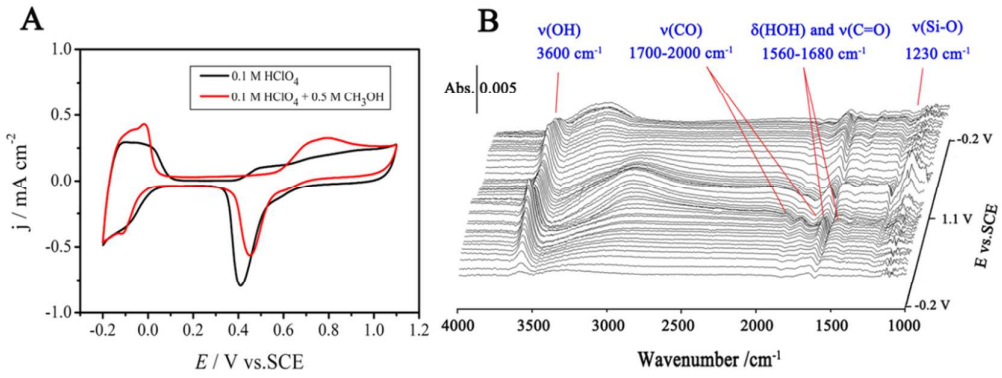

Figure S4. (A) Cyclic voltammograms of a Pd electrode in 0.1 M $HClO_4$ in the absence and presence of 0.5 M CH_3OH at 50 mV/s. (B) In situ ATR-SEIRA spectra acquired while the Pd electrode potential was cycled at 10 mV/s from -0.2 V to 1.1 V and then back to -0.2 V in 0.1 M $HClO_4$ + 0.5 M CH_3OH, the single beam spectrum taken at -0.2 V (SCE) in the same electrolyte as the reference spectrum.

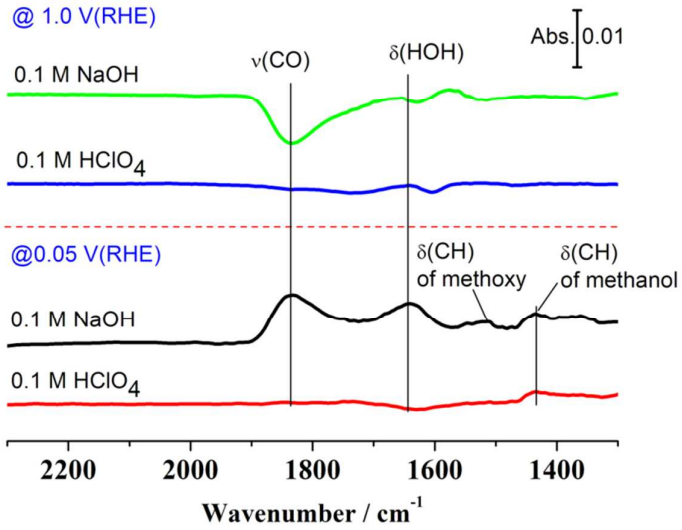

Figure S5. Comparison of IR spectra taken at Pd electrodes in 0.1 M NaOH + 0.5 M CH_3OH and 0.1 M $HClO_4$ + 0.5 M CH_3OH at 0.05 and 1.0 V (RHE). The spectra taken at 0.05 V used the single beam spectrum acquired in 0.1 M NaOH and 0.1 M $HClO_4$ as the reference spectrum, respectively; and the spectra taken at 1.0 V used the single beam spectrum acquired in 0.1 M NaOH + 0.5 M CH_3OH and 0.1 M $HClO_4$ + 0.5 M CH_3OH at 0.05 V as the reference spectrum, respectively.

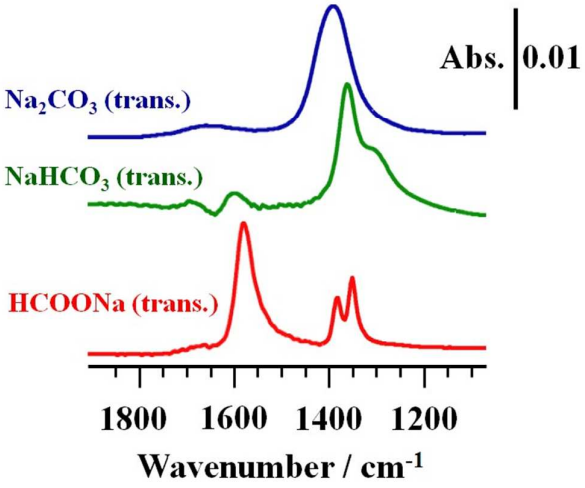

Figure S6. Transmission mode IR spectra of 0.1 M $NaCO_3$, 0.1 M $NaHCO_3$ and 0.1 M HCOONa collected in a 6-μm-thick flow transmission cell.